

Mass Spectrometric and Spectroscopic Studies on Hydrolysis of Phosphoesters by Bis(μ-acetato)-μ-phenolato Dinuclear Metal(II) Complexes (Metal = Mn, Co, Ni, and Zn)

Reiko Jikido, Hitomi Shiraishi, Kanako Matsufuji, Masaaki Ohba,† Hideki Furutachi,[1] Masatatsu Suzuki,[1] and Hisashi Ōkawa*

Department of Chemistry, Faculty of Science, Kyushu University, Hakozaki 6-10-1, Higashi-ku, Fukuoka 812-8581

[1]Department of Chemistry, Faculty of Science, Kanazawa University, Kakuma-machi, Kanazawa 920-1192

Received March 7, 2005; E-mail: okawascc@mbox.nc.kyushu-u.ac.jp

Dinuclear metal(II) complexes of 2,6-bis{*N*-[(2-dimethylamino)ethyl]iminomethyl}-4-methylphenol (HL), $[Mn_2(L)(AcO)_2(NCS)]$ (**1**), $[Co_2(L)(AcO)_2]BPh_4$ (**2**), $[Ni_2(L)(AcO)_2(MeOH)]BPh_4$ (**3**), and $[Zn_2(L)(AcO)_2]BPh_4$ (**4**), have been examined as regards their hydrolytic activity toward tris(*p*-nitrophenyl) phosphate (TNP) and hydrogen bis(*p*-nitrophenyl) phosphate (HBNP) by means of mass spectrometric methods as well as UV–visible spectroscopic methods. All the complexes hydrolyze TNP to BNP^- in the relative activity of **4** > **2** > **1** ≫ **3**. It is found that one AcO^- group of $[M_2(L)(AcO)_2]^+$ is replaced with BNP^-, arising from the hydrolysis of TNP, affording $[M_2(L)(AcO)(bnp)]^+$ in an equilibrium with $[M_2(L)(AcO)_2]^+$: $[M_2(L)(AcO)_2]^+ + BNP^- \rightleftarrows [M_2(L)(AcO)(bnp)]^+ + AcO^-$. In the reaction of HBNP with **1**–**4**, $[M_2(L)(AcO)(bnp)]^+$ is produced in the equilibrium with $[M_2(L)(AcO)_2]^+$, and the bound BNP^- is slowly hydrolyzed in the case of M = Mn and Co. The bound BNP^- of $[Ni_2(L)(AcO)(bnp)]^+$ is barely hydrolyzed and the bound BNP^- of $[Zn_2(L)(AcO)(bnp)]^+$ is practically not hydrolyzed. The relevance of the complexes to phosphotriesterase and phosphodiesterase is discussed.

It is known that dinuclear or trinuclear metal cores exist at the active site of phosphatases.[1–5] Phosphotriesterase[4] has a pair of Zn ions at the active site to facilitate the concerted binding of a phosphotriester on one Zn center and the nucleophilic attack of hydroxide or activated water on the adjacent Zn center. Phosphodiesterases such as phospholipase C[3] and P1 nuclease[5] have three Zn ions at the active site to hydrolyze a phosphodiester. It is supposed that the phosphodiesterases require a trinuclear Zn core to accommodate a bidentate phosphodiester on a dinuclear Zn center and to provide water on the third Zn center. Model studies of phosphotriesterase and phosphodiesterase have been made using synthetic dinuclear and trinuclear Zn complexes.[6–13] Another class of phosphodiesterases has a dinuclear FeFe,[14,15] FeZn,[16–18] FeMn,[19] or MnMn[20] core instead of a trinuclear Zn core. Model studies using homo- and heterodinuclear metal complexes have proposed a mechanistic scheme involving the binding of a phosphodiester on a dinuclear core and the nucleophilic attack of water on one metal center (Fe or Mn).[21–28]

Previously, we reported that $[Zn_2(L)(AcO)_2]PF_6$ (HL = 2,6-bis{*N*-[(2-dimethylamino)ethyl]iminomethyl}-4-methylphenol, Fig. 1) and related dinuclear Zn complexes have a phosphotriesterase-like activity to hydrolyze tris(*p*-nitrophenyl) phosphate (TNP) to bis(*p*-nitrophenyl) phosphate (BNP^-).[11] In the present work, the hydrolysis of TNP to BNP^- and the hydrolysis of BNP^- to mono(*p*-nitrophenyl) phosphate (MNP^{2-}) have been studied using the following dinuclear metal complexes of HL: $[Mn_2(L)(AcO)_2(NCS)]$ (**1**), $[Co_2(L)(AcO)_2]BPh_4$ (**2**), $[Ni_2(L)(AcO)_2(MeOH)]BPh_4$ (**3**), and $[Zn_2(L)(AcO)_2]BPh_4$ (**4**). One of our interests is to see if the dinuclear Mn, Co, and Ni complexes (**1**–**3**) have a phosphotriesterase-like function to hydrolyze TNP to BNP^- as found for $[Zn_2(L)(AcO)_2]PF_6$[11] (PF_6^- salt of **4**). Another interest is to examine phosphodiesterase-like activity to hydrolyze BNP^- to MNP^{2-} with respect to the metal ion of **1**–**4**. In this work, we adopt mass spectrometric method, as well as conventional UV–visible spectroscopic method, with hopes to obtain direct information about the species existing in the reaction solution. Positive and negative ESI mass spectrometric studies have demonstrated the formation of $[M_2(L)(AcO)(bnp)]^+$ as the product in the hydrolysis of TNP and the involvement of this complex species as an intermediate in the hydrolysis of BNP^-.

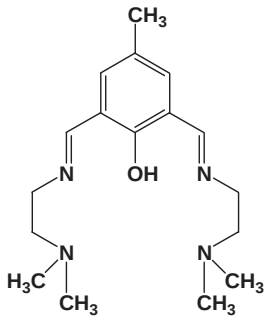

Fig. 1. Chemical structure of HL.

† Present address: Graduate School of Engineering, Department of Synthetic Chemistry and Biological Chemistry, Kyoto University, Katsura, Nishikyo-ku, Kyoto 615-8510

Published on the web October 4, 2005; DOI 10.1246/bcsj.78.1795

Experimental

Synthesis. 2,6-Diformyl-4-methylphenol was prepared by the literature method.[29] Other chemicals were purchased from commercial sources and used without further purification.

$[Mn_2(L)(AcO)_2(NCS)]$ (1). This complex was obtained by the literature method and was identified by IR and UV–visible spectra in comparison with the literature data.[30]

$[Co_2(L)(AcO)_2]BPh_4$ (2). The ligand HL was prepared in situ by reacting 2,6-diformyl-4-methylphenol (0.164 g, 1.00 mmol) and *N*,*N*-dimethylethylenediamine (0.176 g, 2.00 mmol) in hot methanol (10 cm^3). To the ligand solution was added cobalt(II) acetate tetrahydrate (0.498 g, 2.00 mmol), and the mixture was stirred at its boiling temperature for 30 min. The addition of a methanol solution of sodium tetraphenylborate (0.342 g, 1.00 mmol) resulted in the precipitation of brown microcrystals. They were dissolved in chloroform and the solution was diffused with *n*-hexane to give brown crystals. Yield: 72%. Anal. Found: C, 62.95; H, 6.22; N, 6.53; Co, 13.9%. Calcd for $C_{45}H_{53}N_4O_5BCo_2$: C, 62.69; H, 6.16; N, 6.44; Co, 13.7%. Selected IR data [ν/cm^{-1}] using KBr disk: 1649, 1638, 1581, 1441, 734, 707. UV–vis [λ_{max}/nm (ε/$M^{-1}\,cm^{-1}$)] in DMSO–MeCN (1:4 in volume): 245 (13400), 380 (3430), 560_{sh} (ca. 100), 1160 (60).

$[Ni_2(L)(AcO)_2(MeOH)]BPh_4$ (3). This complex was obtained by the literature method and identified by IR and UV–visible spectra in comparison with the literature data.[31]

$[Zn_2(L)(AcO)_2]BPh_4$ (4). This complex was obtained as a yellow powder in a way similar to that for **2** using zinc(II) acetate dihydrate. Yield: 61%. Anal. Found: C, 62.09; H, 6.02; N, 6.53; Ni, 14.6%. Calcd for $C_{45}H_{53}N_4O_5BZn_2$: C, 62.02; H, 6.13; N, 6.43; Zn, 15.0%. Selected IR data [ν/cm^{-1}] using KBr disk: 1652, 1640, 1600, 1446, 735, 708. UV–vis [λ_{max}/nm (ε/$M^{-1}\,cm^{-1}$)] in DMSO–MeCN (1:4 in volume): 249 (13900), 388 (3060).

X-ray Crystallography. A single crystal of **2** was mounted on a glass fiber. Measurements were carried out on a Rigaku/MSC Mercury diffractometer with graphite monochromated Mo Kα radiation at -90 ± 1 °C. Data were collected using CrystalClear program (Rigaku) and corrected for Lorentz and polarization effects. The structures were solved by a direct method and expanded using Fourier technique. The non-hydrogen atoms were refined anisotropically. Hydrogen atoms were included for structure analysis but not refined. All calculations were performed using the teXsan crystallographic software package of Molecular Structure Corporation.[32] Pertinent crystallographic parameters are summarized in Table 1.

Crystallographic data have been deposited at the Cambridge Crystallographic Data Center as supplementary publication No. CCDC 264282. Copies of the data can be obtained free of charge via http://www.ccdc.cam.ac.uk/conts/retrieving.html (or from the Cambridge Crystallographic Data Centre, 12, Union Road, Cambridge, CB2 1EZ, UK; Fax: +44 1223 336033; e-mail: deposit@ccdc.cam.ac.uk).

Mass Spectrometric and Spectroscopic Studies. The hydrolysis of TNP and HBNP by **1**–**4** was studied in a DMSO–MeCN (1:4 in volume) mixed-solvent containing 0.3% (v/v) water at 25 °C. A solution of a complex (**1**–**4**) and a substrate (TNP or HBNP) in the mixed solvent ([complex] = [substrate] = 2.00×10^{-3} M) was prepared and subjected to positive and negative ESI mass spectrometric measurements using a Micromass LCT spectrometer equipped with an iron spray interface. Tetra(octyl)-ammonium perchlorate (2.00×10^{-3} M) was added as the internal standard for positive ESI mass studies. As the internal standard for negative ESI studies tetraphenylborate ion (TPB^-) was used; NaTPB (2.00×10^{-3} M) was added in the reaction with **1**, while TPB^- involved as the counter anion was used in the reaction with **2**–**4**. Observed mass peaks were comprised of some components associated with isotopic atoms. Mass peaks were assigned in agreement down to second places of decimals, by taking into consideration the natural abundance of isotopic atoms. For UV–visible spectroscopic studies, a complex solution in the mixed-solvent (2.00×10^{-3} M) was used as the reference and the difference spectra were measured on a Shimadzu UV-3100PC spectrophotometer.

Table 1. Crystallographic Parameters for $[Co_2(L)(AcO)_2]BPh_4$ (**2**)

Formula	$BC_{45}Co_2H_{53}N_4O_5$
Formula weight	858.61
Crystal system	orthorhombic
Space group	*Pbca* (No. 61)
a/Å	14.8751(6)
b/Å	21.0614(6)
c/Å	27.581(1)
α/°	90.00
β/°	90.00
γ/°	90.00
V/Å^3	8640.9(1)
Z value	8
D_{calcd}/g cm^{-3}	1.320
μ(Mo Kα)/cm^{-1}	8.17
No. observations	9736
R	0.059
Rw	0.103

Other Physical Measurements. Elemental analyses of C, H, and N were obtained at The Service Center of Elemental Analysis of Kyushu University. Metal analyses were obtained on a Shimadzu AA-680 Atomic Absorption/Flame Emission Spectrophotometer. Infrared spectra were recorded using KBr disk on a Perkin Elemer Spectrum BX FT-IR system.

Results and Discussion

Crystal Structures. The structure of **2** is determined in this work. An ORTEP[33] view with the selected atom numbering scheme is shown in Fig. 2. Relevant bond distances and angles are summarized in Table 2.

Two metal ions in the $[Co_2(L)(AcO)_2]^+$ cation are bridged by the phenolic oxygen atom of L^- and two acetate groups in the syn,syn-mode. The Co(1)···Co(2) interatomic separation is 3.216(1) Å. Both Co(1) and Co(2) have a five-coordinate structure. The parameter τ[34] discriminating square-pyramid ($\tau = 0$) and trigonal-bipyramid ($\tau = 1$) is 0.74 for Co(1) and 0.55 for Co(2). Thus, the geometry about Co(1) can be regarded as trigonal-bipyramid with the phenolic oxygen O(1) and the terminal nitrogen N(2) at the axial sites and with the imine nitrogen N(1) and two acetate oxygen atoms O(2) and O(4) on the trigonal base. The geometry about Co(2) is intermediate between square-pyramid and trigonal-bipyramid. The Co(1)-to-donor distances fall in the range of 1.975–2.208 Å and the Co(2)-to-donor distances in the range of 1.979–2.216 Å. The Co(1)–O(1)–Co(2) angle is 102.26(6)°.

The crystal structures of **1**·H_2O·MeOH,[30] **3**,[31] and

Table 2. Selected Bond Distances and Angles of $[Co_2(L)(AcO)_2]BPh_4$ (**2**)

Bond distances/Å			
Co(1)–O(1)	2.064(1)	Co(2)–O(1)	2.066(1)
Co(1)–O(2)	1.975(2)	Co(2)–O(3)	2.002(2)
Co(1)–O(4)	1.980(2)	Co(2)–O(5)	1.979(1)
Co(1)–N(1)	1.996(2)	Co(2)–N(3)	2.003(2)
Co(1)–N(2)	2.208(2)	Co(2)–N(4)	2.216(2)
Co(1)···Co(2)	3.216(1)		
Bond angles/degree			
O(1)–Co(1)–O(2)	92.94(6)	O(1)–Co(2)–O(3)	94.25(6)
O(1)–Co(1)–O(4)	97.18(6)	O(1)–Co(2)–O(5)	97.79(6)
O(1)–Co(1)–N(1)	89.80(6)	O(1)–Co(2)–N(3)	89.85(6)
O(1)–Co(1)–N(2)	170.16(6)	O(1)–Co(2)–N(4)	170.17(6)
O(2)–Co(1)–O(4)	117.49(7)	O(3)–Co(2)–O(5)	113.22(6)
O(2)–Co(1)–N(1)	125.80(7)	O(3)–Co(2)–N(3)	108.29(7)
O(2)–Co(1)–N(2)	89.51(7)	O(3)–Co(2)–N(4)	91.54(6)
O(4)–Co(1)–N(1)	115.79(7)	O(5)–Co(2)–N(3)	136.97(7)
O(4)–Co(1)–N(2)	90.12(7)	O(5)–Co(2)–N(4)	87.19(6)
N(1)–Co(1)–N(2)	81.05(7)	N(3)–Co(2)–N(4)	80.78(6)
Co(1)–O(1)–Co(2)	102.26(6)		

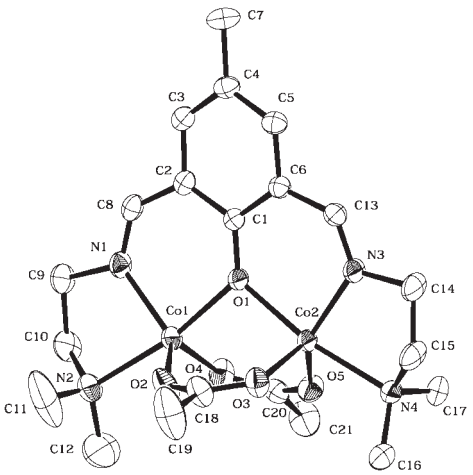

Fig. 2. An ORTEP view of $[Co_2(L)(AcO)_2]BPh_4$ (**2**) with atom numbering scheme.

$[Zn_2(L)(AcO)_2]PF_6$[11] have been determined to have a similar bis(μ-acetato)-μ-phenolato dinuclear core. $\mathbf{1}\cdot H_2O\cdot MeOH$ has a five-coordinate Mn (τ: 0.48) and a six-coordinate Mn with further coordination of thiocyanate-*N* group. Complex **3** has a similar core with a square-pyramidal Ni (τ: 0.17) and a six-coordinate Ni with further coordination of a methanol molecule. Two Zn ions of $[Zn_2(L)(AcO)_2]PF_6$ have a distorted five-coordinate geometry (τ: 0.461 and 0.503).

Phosphoesterase-Like Function. Dimethyl sulfoxide (DMSO) is an appropriate solvent for preparing solutions containing a complex (**1**–**4**) and a substrate (TNP or HBNP). In our preliminary study, however, the DMSO solutions gave ill-resolved mass spectra, probably owing to large polarity and non-volatility of the solvent. The resolution of mass spectra was much improved on adding acetonitrile (MeCN), with small polarity and low boiling point, to the DMSO solutions. Thus, mass spectrometric studies as well as UV–visible spectroscopic studies were carried out in a DMSO–MeCN (1:4 in volume) mixed-solvent containing 0.3% (v/v) water. Complexes **1**–**4** each have an absorption near 380 nm (ε: ca. 3000 $M^{-1}\,cm^{-1}$) attributable to the π–π^* transition of the azomethine linkage of L^-,[35] and this absorption prevents spectroscopic estimation of *p*-nitrophenolate ($\lambda_{max} \sim 420$ nm) arising from the hydrolysis of TNP and HBNP. In the hope of avoiding this problem, spectroscopic studies were carried out using a complex solution in the mixed-solvent (2.00×10^{-3} M, the same complex concentration as that in the reaction solution) as the reference.

Hydrolysis of TNP. UV–visible spectral changes for the TNP hydrolysis by **1**–**4** are given in Fig. 3. The solution with **1** shows complicated features in the ultraviolet region because of the involvement of NCS^-. In the hydrolysis by **1**, **2**, and **4**, the absorption band at 270 nm due to TNP diminished with time, with concomitant increases around 300 and 420 nm; these bands can be attributed to BNP^- and *p*-nitrophenolate, respectively. The spectral change for the TNP hydrolysis by **3** was very slow and the absorption at 420 nm was finally observed after 5 h. The most remarkable feature is the "negative" absorption occurring at 380–410 nm. We presume that complexes **1**–**4** react with BNP^-, arising from the hydrolysis of TNP, producing a BNP-complex and this complex has the azomethine π–π^* transition band at a wavelength different from that of $[M_2(L)(AcO)_2]^+$ ($\sim$380 nm).

The formation of $[M_2(L)(AcO)(bnp)]^+$ in the TNP hydrolysis by **1**–**4** is demonstrated by ESI mass spectrometric studies. Positive ESI mass spectra after completion of time-course are given in Fig. 4. Each positive ESI mass spectrum soon after dissolution (strictly speaking, about 30 s after dissolution owing to machine operation) has a peak due to $[M_2(L)(AcO)_2]^+$: $m/z = 531.12$ for **1**, 539.11 for **2**, 537.11 for **3**, and 549.10 for **4** (the most dominant one of the peak components is used for discussion). In the hydrolysis by **1** and **2**, a weak peak due to $[M_2(L)(AcO)(bnp)]^+$ ($m/z = 811.11$ for M = Mn and $m/z = 819.10$ for M = Co) was recognized within 30 min; this peak did not increase remarkably with time. The peak of

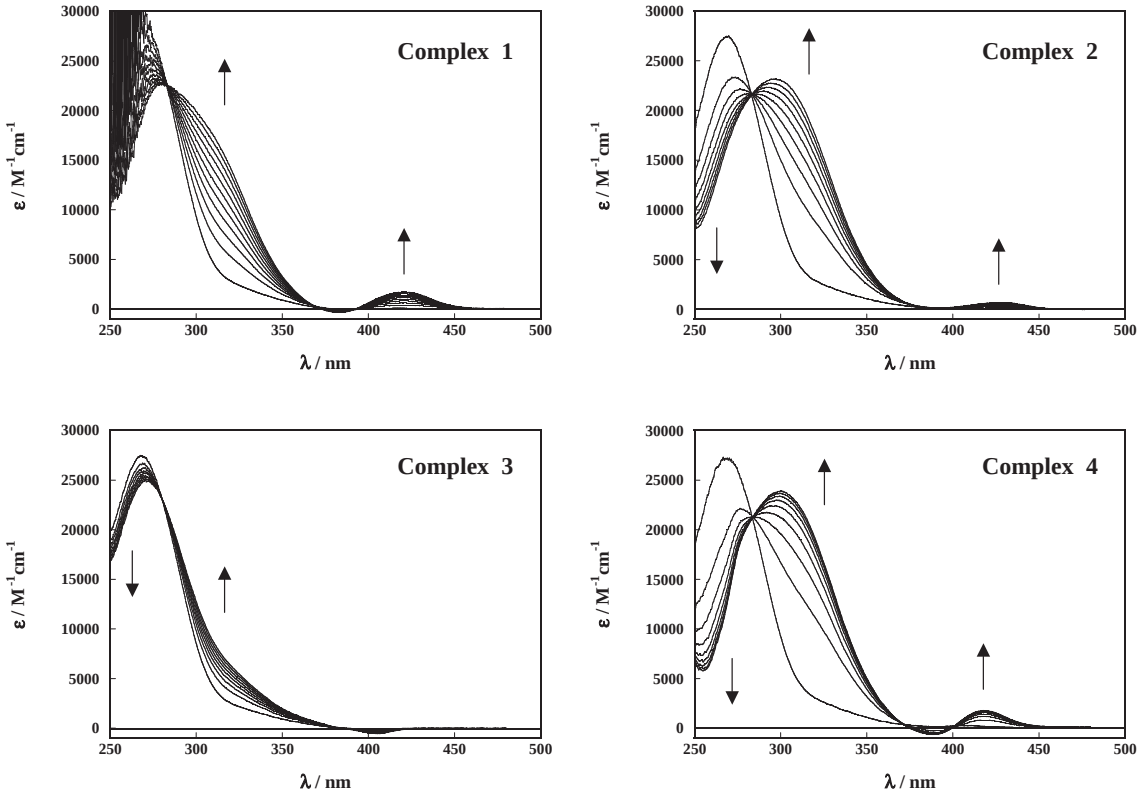

Fig. 3. Difference spectral changes measured every 10 min for TNP hydrolysis by **1**–**4** in DMSO–MeCN (1:4): [complex] = [TNP] = 2.00×10^{-3} M in the reaction solution and [complex] = 2.00×10^{-3} M in the reference solution.

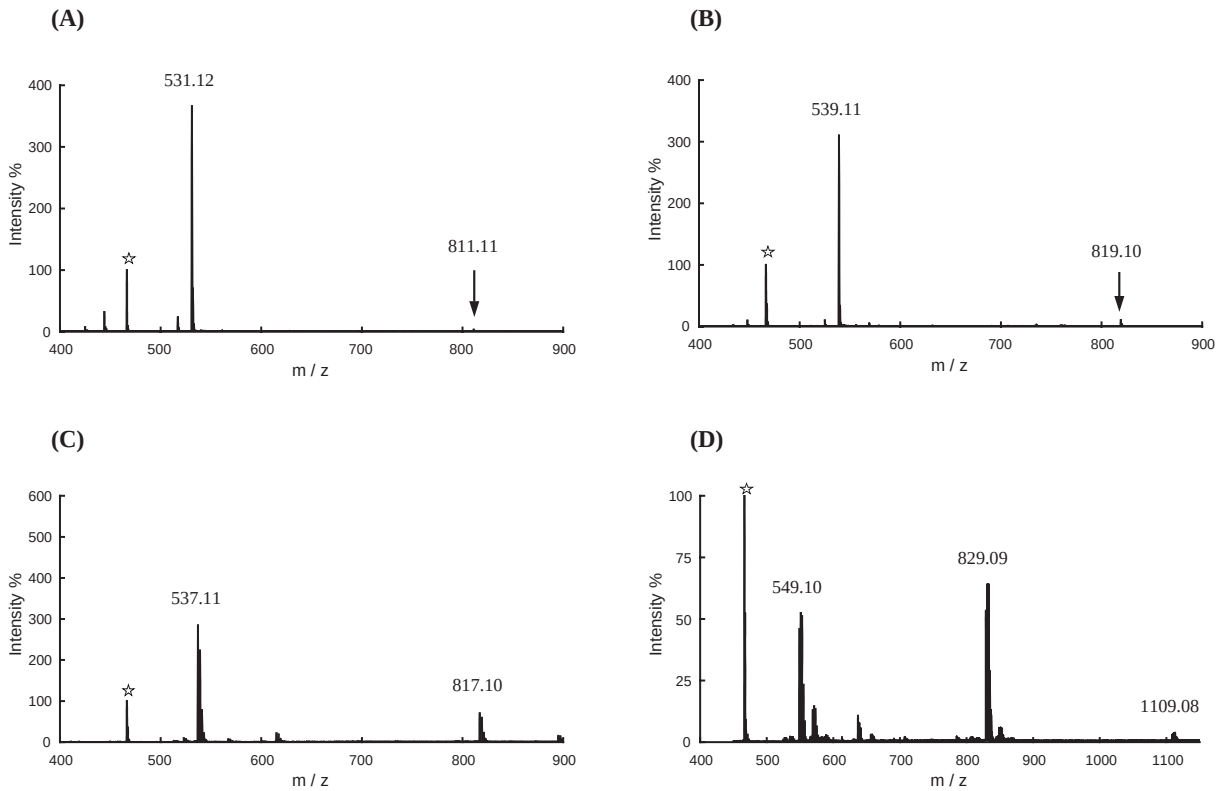

Fig. 4. Positive ESI mass spectra, after termination of time-course, for TNP hydrolysis by **1** (A)–**4** (D) in DMSO–MeCN (1:4) ([complex] = [TNP] = 2.00×10^{-3} M). Time-course terminates in ca. 3 h by **1** (A), in 2 h by **2** (B), in 15 h by **3** (C), and in 1 h by **4** (D). The peak marked with an asterisk is tetra(octyl)ammonium as the internal standard.

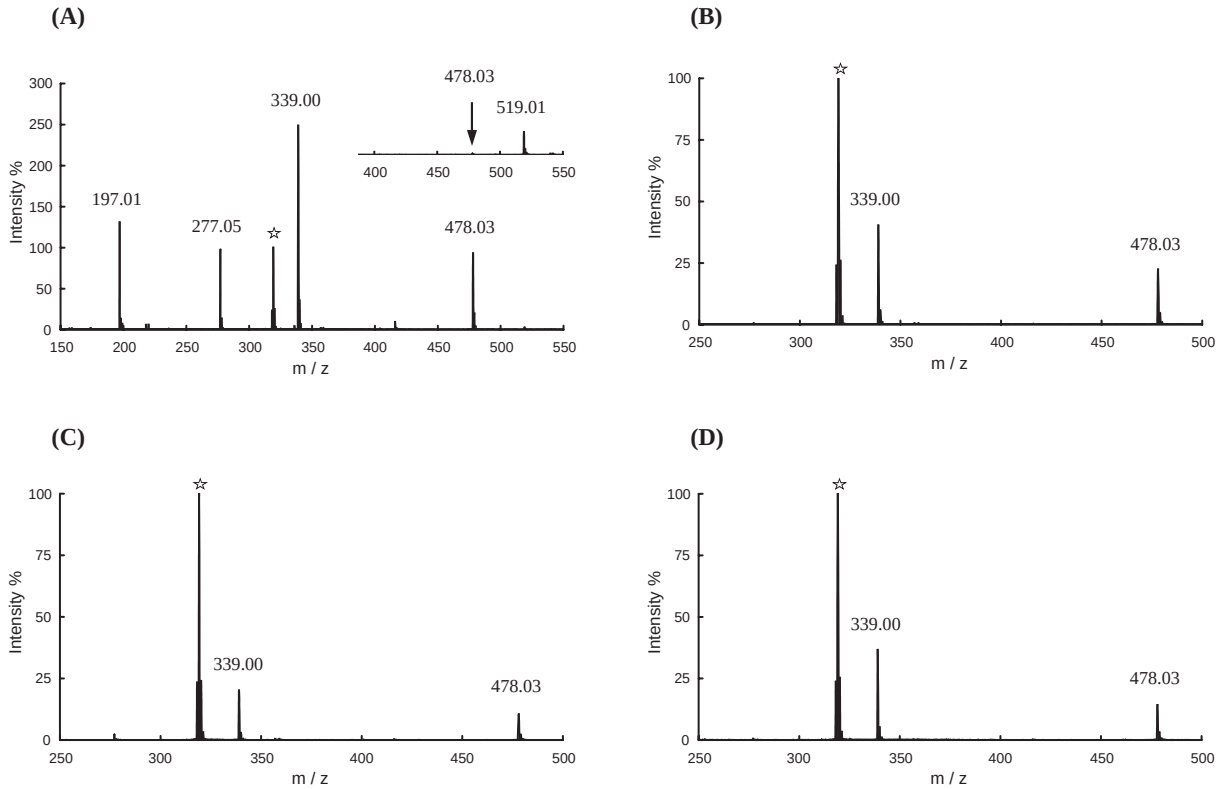

Fig. 5. Negative ESI mass spectra, after termination of time-course, for TNP hydrolysis by **1** (A)–**4** (D) in DMSO–MeCN (1:4) ([complex] = [TNP] = 2.00×10^{-3} M). Time-course terminates in ca. 3 h by **1** (A), in 2 h by **2** (B), in 15 h by **3** (C), and in 1 h by **4** (D). The insert in (A) is the mass spectrum obtained soon after dissolution. The peak marked with an asterisk is PF_6^- as the internal standard.

$[Ni_2(L)(AcO)(bnp)]^+$ ($m/z = 817.10$) in the TNP hydrolysis by **3** was recognized after about 5 h and this peak gradually increased with time to reach a considerable height after 15 h. In the hydrolysis by **4**, the peak of $[Zn_2(L)(AcO)(bnp)]^+$ ($m/z = 829.09$) was recognized soon after dissolution and this peak increased quickly with time to reach a large height in 1 h. In this case, the peak due to $[Zn_2(L)(bnp)_2]^+$ ($m/z = 1109.08$) was also recognized. We suppose that the $[M_2(L)(AcO)(bnp)]^+$ complex has a μ-acetato-μ-bnp dinuclear structure, since the bridging function of BNP^- is well known.[36–40]

Negative ESI mass spectra, after completion of time-course, for the TNP hydrolysis by **1**–**4** are given in Fig. 5. In the hydrolysis by **1**, a peak due to the adduct, $\{TNP + NCS\}^-$ ($m/z = 519.01$), was observed soon after dissolution (see Insert) along with peaks at $m/z = 197.01$, 277.05, 339.00, and 478.03; these peaks are assigned to $\{p$-nitrophenol + NCS$\}^-$, $\{p$-nitrophenol + p-nitrophenolate$\}^-$, BNP^-, and $\{BNP + p$-nitrophenol$\}^-$, respectively. The peak of $\{TNP + NCS\}^-$ diminished with time and finally disappeared in 3 h, while the peaks of $\{p$-nitrophenol + NCS$\}^-$, $\{p$-nitrophenol + p-nitrophenolate$\}^-$, BNP^-, and $\{BNP + p$-nitrophenol$\}^-$ increased with time to reach a steady height in 3 h. Thus, TNP is completely hydrolyzed in 3 h in this reaction.

The negative ESI mass spectra for the hydrolysis by **2**–**4** are simplified because of the absence of NCS^- in the reaction solution. In the hydrolysis by **2** and in the hydrolysis by **4**, weak peaks due to BNP^- ($m/z = 339.00$) and $\{BNP + p$-nitrophenol$\}^-$ ($m/z = 478.03$) were recognized soon after dissolution. These peaks increased with time to reach a steady height in 2 h for the hydrolysis by **2** and in 1 h for the hydrolysis by **4**. In the hydrolysis by **3**, no prominent peak was observed soon after dissolution, but the peaks of BNP^- and $\{BNP + p$-nitrophenol$\}^-$ were recognized after 5 h and these peaks gradually increased with time to reach a steady height after 15 h.

These ESI mass spectrometric results demonstrate the hydrolysis of TNP by **1**–**4** to afford $[M_2(L)(AcO)(bnp)]^+$ in an equilibrium with $[M_2(L)(AcO)_2]^+$. The hydrolysis may be promoted by the nucleophilic attack of water on one metal center to the phosphorus nucleus of TNP on the adjacent metal center (Fig. 6); the release of BNP^- produces $[M_2(L)(AcO)_2]^+$ or the release of AcO^- produces $[M_2(L)(AcO)(bnp)]^+$. Irrespective of the mechanism producing different complex species, the following equilibrium is established, as evidenced by the reaction of HBNP with **1**–**4** in next section: $[M_2(L)(AcO)_2]^+ + BNP^- \rightleftarrows [M_2(L)(AcO)(bnp)]^+ + AcO^-$. Despite limitations of mass spectrometry in qualitative treatment, the apparent $[M_2(L)(AcO)(bnp)]/[M_2(L)(AcO)_2]$ ratios are estimated to be 1/100 with **1**, 1/70 with **2**, 3/7 with **3**, and 3/2 with **4** from the peak heights of two complex ions. Based on the apparent ratio, the spectral change with **1** and that with **2** in Fig. 3 are mostly concerned with the hydrolysis of TNP, whereas the spectral change with **3** and that with **4** are concerned with both the hydrolysis of TNP and the equilibration between $[M_2(L)(AcO)^2]^+$ and $[M_2(L)(AcO)(bnp)]^+$. Evidently the negative absorption at 380–410 nm arises from a balance of the spectrum of $[M_2(L)(AcO)(bnp)]^+$ produced in the reaction so-

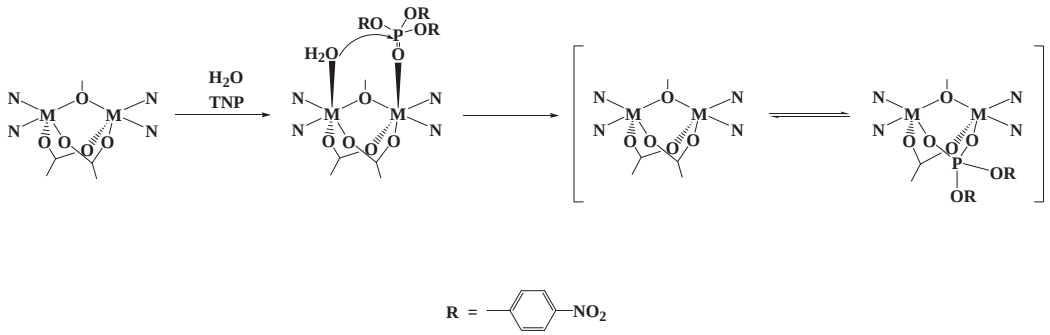

Fig. 6. Mechanistic scheme for hydrolysis of TNP by **1**–**4**.

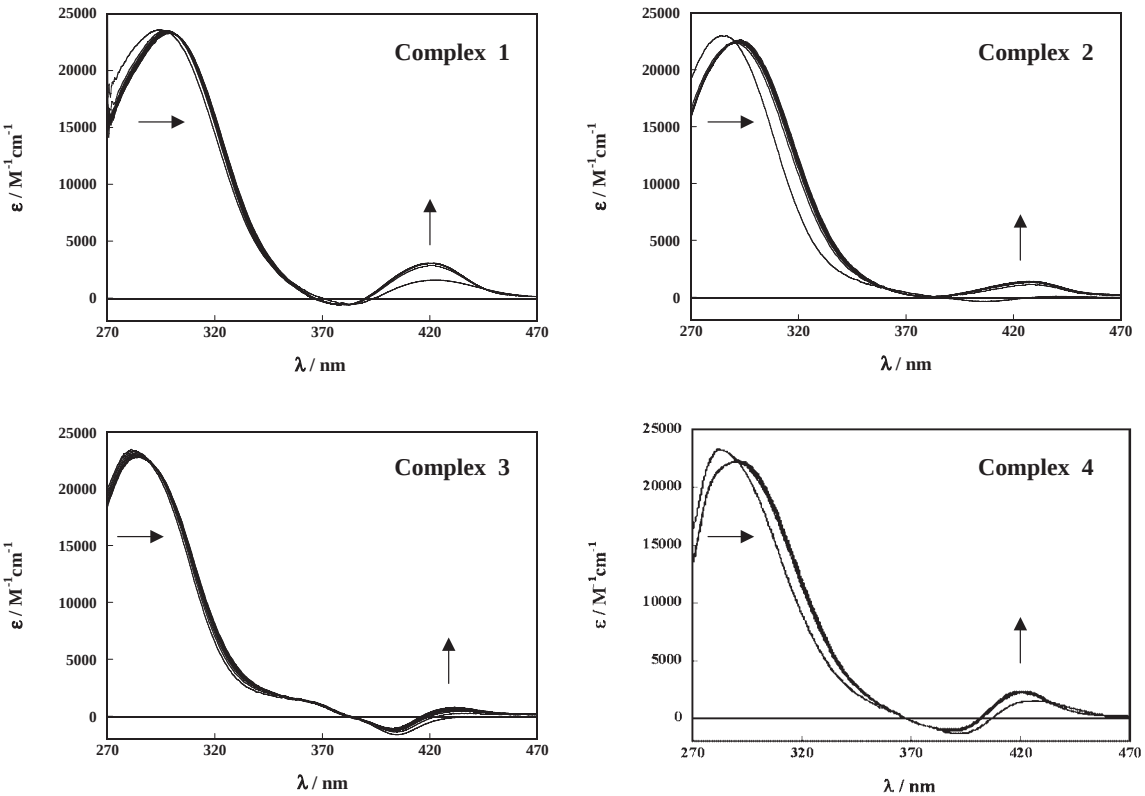

Fig. 7. Difference spectral changes measured every 10 min for HBNP hydrolysis by **1**–**4** in DMSO–MeCN (1:4): [complex] = [HBNP] = 2.00×10^{-3} M in the reaction solution and [complex] = 2.00×10^{-3} M in the reference solution.

lution and the spectrum of $[M_2(L)(AcO)_2]^+$ as the reference. Comparisons of the spectra of Fig. 3 with the spectra of **1**–**4** show that $[M_2(L)(AcO)(bnp)]^+$ has the π–π^* transition band associated with the ligand C=N linkage at 390–420 nm. Since the characteristic absorption of *p*-nitrophenolate is at 420 nm, visible spectroscopy cannot be applied to the hydrolysis of TNP.

The positive and negative ESI mass spectra for the TNP hydrolysis converged in 3 h with **1**, in 2 h with **2**, in 15 h with **3**, and in 1 h with **4**. Thus, the relative order in phosphotriesterase-like activity of **4** > **2** > **1** ≫ **3** can be deduced. The high hydrolytic activity of **4** toward TNP illustrates the preference of a dinuclear Zn core at the active site of phosphotriesterase. The low activity of **3** to hydrolyze TNP is notable. It is likely that the water bound to Ni(II) has low nucleophilicity because of the large electronegativity of Ni^{2+} ion relative to Mn^{2+}, Co^{2+}, and Zn^{2+} ions.[41]

Hydrolytic Function toward HBNP. UV–visible spectral changes with time for the reaction of HBNP with **1**–**4** are given in Fig. 7. The hydrolysis of BNP^- to MNP^{2-} is accompanied by only a small change in the near ultraviolet region, because BNP^- and MNP^{2-} have their characteristic absorption band at close wavelengths.[25] The visible spectral feature with negative absorption near 370–400 nm suggests a fast reaction of HBNP with **1**–**4** producing $[M_2(L)(AcO)(bnp)]^+$ in an equilibrium with $[M_2(L)(AcO)_2]^+$. In fact, the positive ESI mass spectra for the reaction of HBNP with **1**–**4** (soon after dissolution) resemble the mass spectra for the TNP hydrolysis by **1**–**4** in Fig. 4, respectively. That is, the equilibrium for the reaction of HBNP by **1**–**4** is essentially the same as that established for the hydrolysis of TNP by **1**–**4**, respectively.

The negative ESI mass spectra after 15 h for the reaction of

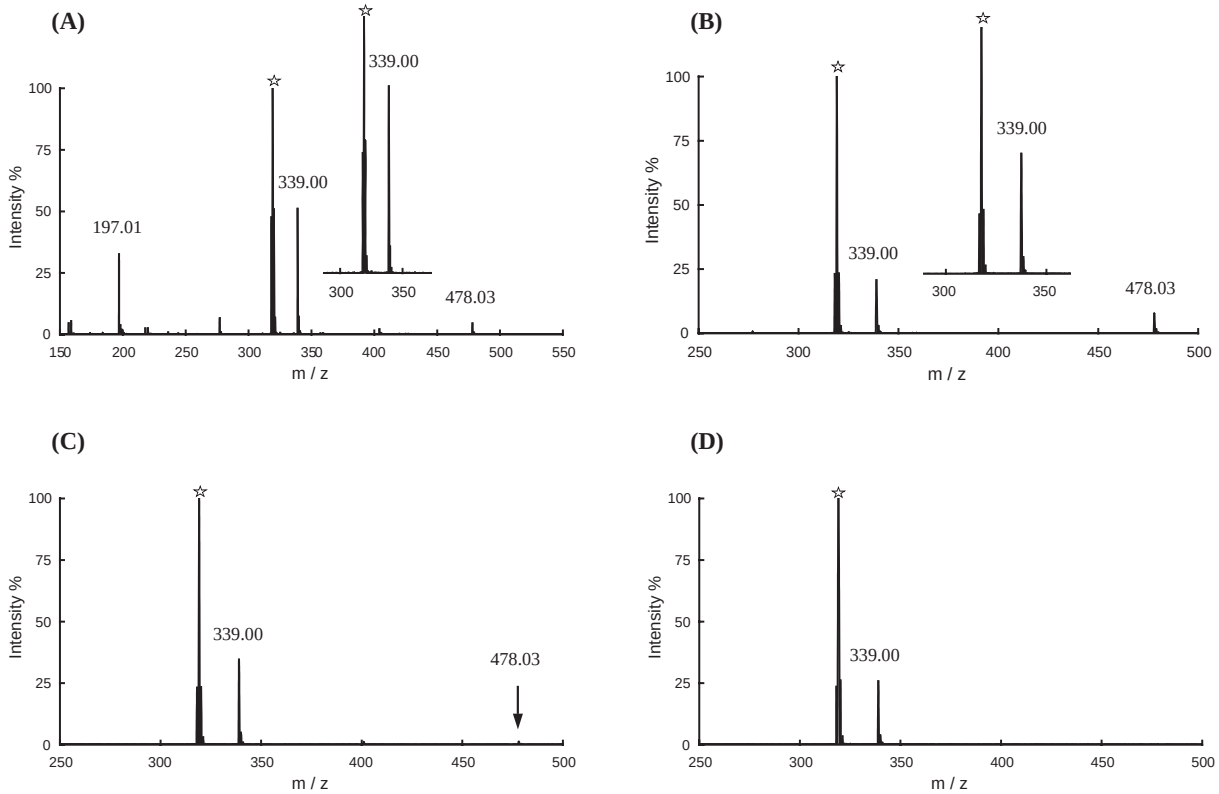

Fig. 8. Negative ESI mass spectra after 15 h for the reaction of HBNP with **1** (A)–**4** (D) in DMSO–MeCN (1:4) ([complex] = [HBNP] = 2.00×10^{-3} M). The insert in (A) and that in (B) are ESI mass spectra obtained soon after dissolution. The peak marked with an asterisk is PF_6^- as the internal standard.

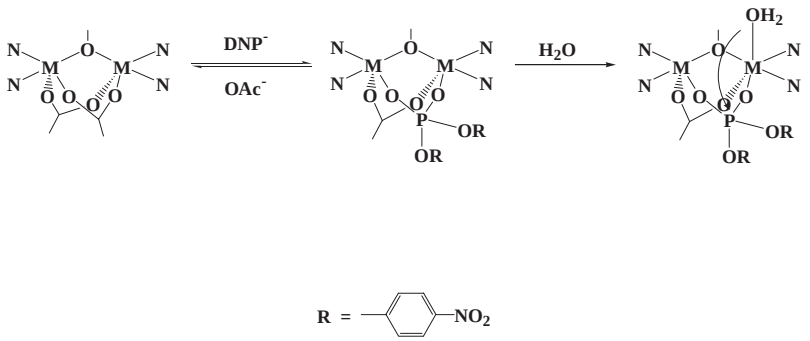

Fig. 9. Mechanistic scheme for hydrolysis of BNP^- by **1**–**3**.

HBNP with **1**–**4** are given in Fig. 8. Each mass spectrum soon after dissolution has one peak due to BNP^- ($m/z = 339.00$). In the reaction with **1**, the relative intensity of the peak gradually decreased with time with concomitant occurrence of two peaks due to {*p*-nitrophenol + NCS}$^-$ ($m/z = 197.01$) and {*p*-nitrophenol + *p*-nitrophenolate}$^-$ ($m/z = 478.03$). In the reaction with **2**, the peak of BNP^- gradually decreased with time with concomitant occurrence of the peak of {BNP + *p*-nitrophenol}$^-$ ($m/z = 478.03$). Thus, **1** and **2** hydrolyze HBNP through $[M_2(L)(AcO)(bnp)]^+$. In the reaction with **3**, the decrease in the peak of BNP^- was not obvious but a very weak peak due to {BNP + *p*-nitrophenol}$^-$ was found after 15 h. In the reaction with **4**, the peak of BNP^- remained intact and no peak due to {BNP + *p*-nitrophenol}$^-$ was detected after 15 h. Thus, the bound BNP^- of $[Ni_2(L)(AcO)(bnp)]^+$ is barely hydrolyzed and the bound BNP^- of $[Zn_2(L)(AcO)(bnp)]^+$ is not hydrolyzed. It should be mentioned that the absorption occurring at ~420 nm in Fig. 7 is evidently fictitious.

Thus, complexes **1**–**4** react with HBNP to afford $[M_2(L)(AcO)(bnp)]^+$ in an equilibrium with $[M_2(L)(AcO)_2]^+$. The bound BNP^- of $[M_2(L)(AcO)(bnp)]^+$ (M = Mn and Co) may be hydrolyzed through the intermediate $[M_2(L)(AcO)(bnp)(H_2O)]^+$ that allows the nucleophilic attack of water to the phosphorus nucleus of the bridging BNP^- (Fig. 9). The hydrolytic activity of **1** toward HBNP illustrates the significance of dinuclear Mn in phosphodiesterase.[20] The present result suggests that dinuclear Co complex can have a phosphodiesterase-like activity, but Co is not preferred for phosphodiesterase probably because of its low abundance in sea water. It must be emphasized that **4** has little activity to hydrolyze BNP^- in con-

trast to its high activity to hydrolyze TNP. It appears that dinuclear Zn core cannot easily accept a water molecule when bridged by BNP^-, and this explains why Zn-based phosphodiesterases requires the third Zn for biological function.[3,5] Recently, we succeeded in obtaining $[M_2(L)(bnp)_2(H_2O)]BNP$ (M = Co and Ni) and $[Zn_2(L)(bnp)_2]ClO_4$ by a reaction of **2**–**4** with excess HBNP.[42] The absence of water in the Zn complex can be taken as a support to our presumption that dinuclear Zn core bridged by BNP^- accepts water with great difficulty. The bound BNP^- of $[M_2(L)(bnp)_2(H_2O)]BNP$ (M = Co and Ni) and $[Zn_2(L)(bnp)_2]ClO_4$ is not hydrolyzed in hydrous DMSO. Thus, we may conclude that the hydrolysis of TNP by **1**–**4** and the hydrolysis of HBNP by **1** and **2** are stoichiometric but not catalytic.

Conclusion

ESI mass spectrometry has applied to the study of hydrolysis of TNP and HBNP by $[Mn_2(L)(AcO)_2(NCS)]$ (**1**), $[Co_2(L)(AcO)_2]BPh_4$ (**2**), $[Ni_2(L)(AcO)_2(MeOH)]BPh_4$ (**3**), and $[Zn_2(L)(AcO)_2]BPh_4$ (**4**). All the complexes hydrolyze TNP to BNP^- affording $[M_2(L)(AcO)(bnp)]^+$ in an equilibrium with $[M_2(L)(AcO)_2]^+$; $[M_2(L)(AcO)_2]^+ + BNP^- \rightleftarrows [M_2(L)(AcO)(bnp)]^- + AcO^-$. The $[M_2(L)(AcO)(bnp)]^+/[M_2(L)(AcO)_2]^+$ ratio in the equilibrium is estimated to be 1/100 for with **1**, 1/70 with **2**, 3/7 with **3**, and 3/2 with **4**. The hydrolytic activity of the complexes decreases in the order of **4** > **2** > **1** ≫ **3**. A high activity of **4** to hydrolyze TNP illustrates the preference of a dinuclear Zn core at the active site of phosphotriesterase. In the reaction of HBNP with **1**–**4**, one AcO^- group of $[M_2(L)(AcO)_2]^+$ is replaced with BNP^-, affording $[M_2(L)(AcO)(bnp)]^+$ in the equilibrium with $[M_2(L)(AcO)_2]^+$. The bound BNP^- of $[M_2(L)(AcO)(bnp)]^+$ (M = Mn and Co) is slowly hydrolyzed, whereas the bound BNP^- of $[Ni_2(L)(AcO)(bnp)]^+$ is barely hydrolyzed and the bound BNP^- of $[Zn_2(L)(AcO)(bnp)]^+$ is not hydrolyzed. The present result is in harmony with the general observation that a dinuclear Mn core exists at the active site of a phosphodiesterase (protein phophatase 2C) and Zn-based phosphatases have a trinuclear Zn core but not a dinuclear Zn core. Complex **3** has a low activity to hydrolyze TNP and only a little activity to hydrolyze HBNP owing to the poor nucleophilicity of the water bound to Ni(II). Conventional spectroscopic methods cannot be applied to the present study, because of the equilibration between $[M_2(L)(AcO)_2]^+$ and $[M_2(L)(AcO)(bnp)]^+$.

References

1 D. E. Fenton and H. Ōkawa, "Perspectives on Bioinorganic Chemistry," JAI Press, London (1993), Vol. 2, p. 81; J. L. Vanhooke, M. M. Benning, F. M. Raushel, and H. M. Holden, *Biochemistry*, **35**, 6020 (1996).

2 E. Hough, L. K. Hansen, B. Birkness, K. Jynge, S. Hansen, A. Hardvik, C. Little, E. J. Dodson, and Z. Derewenda, *Nature*, **338**, 357 (1989).

3 J. L. Vanhooke, M. M. Benning, F. M. Raushel, and H. M. Holden, *Biochemistry*, **35**, 6020 (1996).

4 A. Lahm, S. Volbeda, F. Sakijama, and D. Suck, *J. Mol. Biol.*, **215**, 207 (1990).

5 W. H. Chapman, Jr. and R. Breslow, *J. Am. Chem. Soc.*, **117**, 5462 (1995).

6 T. Koike, M. Inoue, E. Kimura, and M. Shiro, *J. Am. Chem. Soc.*, **118**, 3091 (1996).

7 P. Molenveld, S. Kapsabelis, J. F. J. Engbersen, and D. N. Reinhoudt, *J. Am. Chem. Soc.*, **119**, 2948 (1997).

8 P. Molenveld, W. M. G. Stikvoort, H. Kooijman, A. L. Spek, J. F. J. Engbersen, and D. N. Reinhoud, *J. Org. Chem.*, **64**, 3896 (1999).

9 C. Bazzicalupi, A. Bencini, A. Bianchi, V. Fusi, C. Giorgi, P. Paoletti, B. Valtancoli, and D. Zanchi, *Inorg. Chem.*, **36**, 2784 (1997).

10 K. Abe, J. Izumi, M. Ohba, T. Yokoyama, and H. Ōkawa, *Bull. Chem. Soc. Jpn.*, **74**, 85 (2001).

11 M. Yashiro, A. Ishikubo, and M. Komiyama, *J. Chem. Soc., Chem. Commun.*, **1995**, 1793.

12 M. Yashiro, A. Ishikubo, and M. Komiyama, *J. Chem. Soc., Chem. Commun.*, **1997**, 83.

13 E. E. Kim and H. W. Wyckoff, *J. Mol. Biol.*, **218**, 449 (1991).

14 L. Que, Jr. and A. E. True, *Prog. Inorg. Chem.*, **38**, 91 (1990).

15 T. Klabunde, N. Strater, R. Frolich, H. Witzel, and B. Krebs, *J. Mol. Biol.*, **259**, 737 (1996).

16 S. K. Burley, R. R. David, R. M. Sweet, A. Taylor, and W. N. Lipscomb, *J. Mol. Biol.*, **224**, 113 (1992).

17 C. R. Kissinger, H. E. Parge, D. R. Knighton, C. T. Lewis, L. A. Pelletier, A. Tempczyk, V. J. Kalish, K. D. Tucker, R. E. Showalter, E. W. Moomaw, L. N. Gastinel, N. Habuka, X. Chen, F. Maldonado, J. E. Barker, R. Bacquet, and E. Villafranca, *Nature*, **378**, 641 (1995).

18 M. P. Engloff, P. T. W. Cohen, P. Reinemer, and D. Barford, *J. Mol. Biol.*, **254**, 942 (1995).

19 J. Goldberg, H. Huang, Y. Kwon, P. Greengard, A. C. Nairn, and J. Kuriyan, *Nature*, **376**, 745 (1995).

20 A. K. Das, N. R. Helps, P. T. W. Cohen, and D. Barford, *EMBO J.*, **15**, 6798 (1996).

21 E. Bernard, S. Chardon-Noblat, A. Deronzier, and J.-M. Latour, *Inorg. Chem.*, **38**, 190 (1999).

22 F. Verge, C. Lebrum, M. Fontecave, and S. Ménage, *Inorg. Chem.*, **42**, 499 (2003).

23 D. H. Vance and A. W. Czarnik, *J. Am. Chem. Soc.*, **115**, 12165 (1993).

24 M. J. Yound and J. Chin, *J. Am. Chem. Soc.*, **117**, 10577 (1995).

25 H. Machinaga, K. Matsufuji, M. Ohba, M. Kodera, and H. Ōkawa, *Chem. Lett.*, **2002**, 716.

26 M. Lanznaster, A. Neves, A. J. Bortoluzzi, B. Szpoganicz, and E. Schwingel, *Inorg. Chem.*, **41**, 5641 (2002).

27 M. Yamami, H. Furutachi, T. Yokoyama, and H. Ōkawa, *Inorg. Chem.*, **37**, 6832 (1998).

28 K. Arimura, M. Ohba, T. Yokoyama, and H. Ōkawa, *Chem. Lett.*, **2001**, 1134.

29 D. A. Denton and H. Suschitzky, *J. Chem. Soc.*, **1963**, 4741.

30 H. Sakiyama, H. Tamaki, K. Kodera, N. Matsumoto, and H. Ōkawa, *J. Chem. Soc., Dalton Trans.*, **1993**, 591.

31 T. Koga, H. Furutachi, H. Nakamura, N. Fukita, M. Ohba, K. Takahashi, and H. Ōkawa, *Inorg. Chem.*, **37**, 989 (1998).

32 "teXsan Crystal Structure Analysis Package," Molecular Structure Corporation, Houston, TX (1985 and 1999).

33 C. K. Johnson, Report 3794, Oak Ridge National Laboratory, Oak Ridge, TN (1965).

34 A. W. Addison, T. N. Rao, J. Reedaijk, J. V. Rijn, and

G. C. Verschoor, *J. Chem. Soc., Dalton Trans.*, **1984**, 1349.
35 a) B. Bosnich, *J. Am. Chem. Soc.*, **90**, 627 (1968). b) R. S. Downing and F. L. Urbach, *J. Am. Chem. Soc.*, **91**, 5977 (1969).
36 M. Yamami, H. Furutachi, T. Yokoyama, and H. Ōkawa, *Inorg. Chem.*, **37**, 6832 (1998).
37 C. Bazzicalupi, A. Bencini, A. Bianchi, V. Fusi, C. Giorgi, P. Paoletti, B. Valtancoli, and D. Zanchi, *Inorg. Chem.*, **36**, 2784 (1997).
38 K. Schepers, B. Bremer, B. Krebs, G. Henkel, E. Althaus, B. Mosel, and W. Müller-Warmuth, *Angew. Chem., Int. Ed. Engl.*, **29**, 531 (1990).
39 T. Tanase, J. W. Yun, and S. J. Jippard, *Inorg. Chem.*, **35**, 3585 (1996).
40 C. He and S. J. Lippard, *J. Am. Chem. Soc.*, **122**, 184 (2000).
41 A. L. Allred, *J. Inorg. Nucl. Chem.*, **17**, 215 (1961).
42 R. Jikido, Master Thesis of Faculty of Science, Kyushu University (2004). Manuscript has been prepared for publication.